AJP

ISSN : 0971 - 3093

Vol 31, Nos 3 - 6, March - June, 2022

ASIAN JOURNAL OF PHYSICS

An International Peer Reviewed Research Journal

Advisory Editors : W Kiefer, & FTS Yu, Maria J Yzuel

Special issue dedicated to Prof Bishnu P Pal

Prof B P Pal

Guest Editor : Partha Roy Chaudhuri

ap

ANITA PUBLICATIONS

FF-43, 1st Floor, Mangal Bazar, Laxmi Nagar, Delhi-110 092, India

B O : 2, Pasha Court, Williamsville, New York-14221-1776, USA

Asian Journal of Physics
Vol. 31, Nos 3-6 (2022) 465-473
Available on: www.asianjournalofphysics.com

ap

Far-detuned parametric sidebands via multiple intermodal four-wave mixing in communication fiber

Sudip K Chatterjee[1] and R Vijaya[2]

[1]*Department of Physics, Bennett University, Greater Noida-201 310, India*

[2]*Department of Physics and Centre for Lasers and Photonics,*

Indian Institute of Technology Kanpur, Kanpur-208 016, India

Dedicated to Professor Bishnu P Pal for his enormous contributions to the advancement of research and education in science and technology through his unique vision and outstanding dedication

We present a detailed investigation of multiple intermodal four-wave mixing (IMFWM) in the standard communications-grade fiber when it is pumped in the deep normal dispersion regime with Q-switched nanosecond pulses at 532 nm. A brief theoretical analysis based on coupled nonlinear Schrödinger equation under quasi-cw approximation, considering different modes for pumping, is carried out to identify all the allowed phase-matched Stokes and anti-Stokes waves having degenerate and non-degenerate mode configurations. With the first-order anti-Stokes thus generated as the secondary pump, the cascaded IMFWM can produce discrete emission in the ultraviolet range near 390 nm.

Keywords: Four-wave mixing, Parametric Process, Nonlinear Schrödinger equation, Phase-matching.

1 Introduction

Studies on the nonlinear phenomenon of four-wave mixing (FWM) in optical fibers are known since the first demonstration by Stolen *et al* in 1974 [1]. An efficient conversion of pump power to the energy and phase-matched Stokes (red-shifted) and anti-Stokes (blue-shifted) lines in FWM has led to its wide range of applications in supercontinuum (SC) generation, parametric amplification, entangled photon pair generation, and quantum-state-preserving frequency conversion [2-5]. In conventional fiber-optic FWM, which is studied in single-mode fibers, multimode fibers, and the specialty photonic crystal fiber (PCF), it is commonly seen that the pump, Stokes and anti-Stokes waves propagate in the same fiber mode [6,7]. In these cases, the pump wavelength is chosen close to the zero-dispersion wavelength (ZDW) in the anomalous dispersion regime, and the wavelength of the photons in FWM lie close to the pump [8]. Hence, the presence of discrete Stokes and anti-Stokes waves would be severely contaminated by ZDW-dependent SC generation [2]. While utilizing the single-mode FWM for correlated photon pair generation, the coincidental counts of the entangled photons at the detectors would also be affected due to residual pump photons and spontaneous Raman scattered photons (bandwidth ~50 THz) [9]. One way of resolving this issue is by pumping near the ZDW in the normal dispersion regime of specially designed PCF [10,11]. An alternate way is to pump in the deep normal dispersion (no SC contamination) and fulfill the phase-matching condition using different fiber modes in a multimode fiber via a process known as intermodal four-wave mixing (IMFWM) [12-19]. In this process, the generated spectral components would be widely separated from the pump owing to the difference of propagation constants of participating modes. The large spectral shift also makes this technique suitable for the production and control of pure photon pair from highly entangled to factorable state [18].

Corresponding author
e mail: rvijaya@iitk.ac.in (R Vijaya)

Interestingly, the generation of an ensemble of wavelengths and modes through IMFWM has implications for building hyper-entangled sources for quantum communications [20]. In fact, experimental demonstration of far-detuned, frequency converted source in the ultraviolet regime via an advanced cascaded-IMFWM (C-IMFWM) process has been reported in the recent past. Double-clad higher order mode fiber [20], graded-index multimode fiber [21] and photonic crystal fiber [22] are among the host fibers which have been utilized to observe the above phenomenon. However, the combination of high-power mode-locked pump source and specialty host fiber makes the system complex, costly and difficult to integrate in all-fiber configuration. In this paper, we explore the occurrence of multiple IMFWM in a commercial-grade communication fiber by pumping in the deep normal dispersion regime. A brief theoretical analysis that governs all possible intermodal phase matching conditions considering the same or different pump-mode excitation, is discussed. The cascaded intermodal four wave mixing phenomena under secondary pumping scheme to generate a source in the ultraviolet band is also discussed.

2 Our earlier experimental work on IMFWM

Fascinated with this intermodal phase matching phenomena, we have explored the feasibility of generating multiple wavelengths experimentally by utilizing the commercial grade communication fibers [23,24]. Figure 1 depicts the experimental setup for investigating the IMFWM in SMF-28 fiber under Q-switched frequency-doubled Nd:YAG pumping. The laser pulse duration of 7 ns and repetition rate of 10 Hz is used in the experiment. The second harmonic pump at 532 nm is first passed through a variable attenuator (comprising of two polarizers P_A & P_B) and a half-wave plate (HWP). Then, the pump pulses are coupled through a 20× microscope objective (MO) into a Corning SMF-28e+ fiber. The output of the fiber is connected to a spectrometer (USB-4000, Ocean Optics) in the range of 200-900 nm. The modal content of the output beam profile is extracted by using a set of 10 nm band-pass filters (BPF) and a CCD camera. The fiber supports four modes (V~5.7) at the pump wavelength. However, as an essential condition of observing IMFWM, a careful alignment of pump into only the fundamental mode (LP_{01}) of the fiber is achieved by altering the injection conditions. From a series of experiments with various segments of fiber and pump power, the optimized segment of 51 cm SMF-28e+ shows the generation of multiple wavelengths distinctly separated from the pump wavelength.

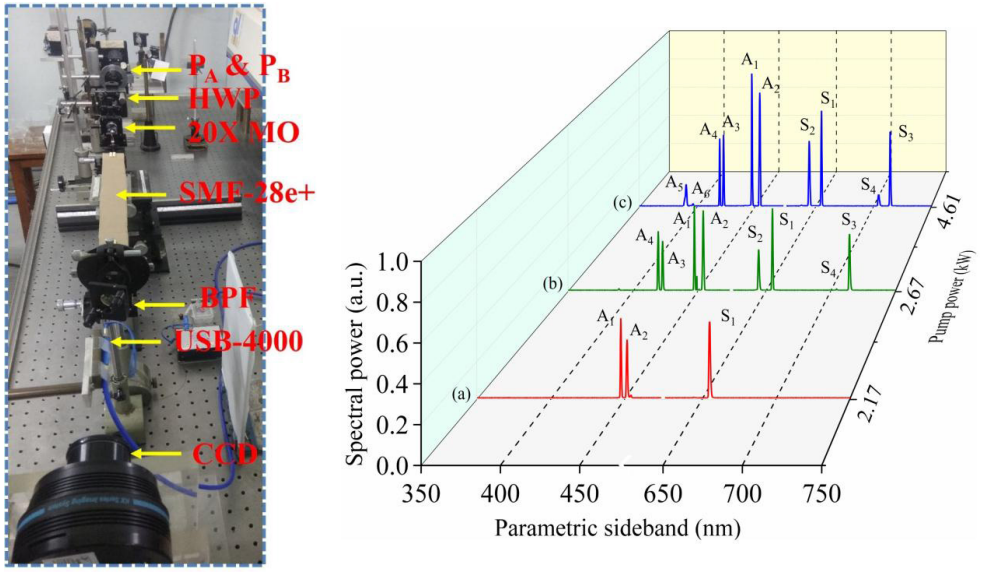

Fig 1. (a) Experimental setup (b) Observed output spectra of 51 cm SMF-28e+ under deep normal dispersion pumping.

Figure 1b depicts three spectra measured from a 51 cm long fiber sample at pump powers (P_P) of 2.17 kW, 2.67 kW and 4.61 kW. Interestingly, here we have witnessed the appearance of four pairs of spectral peaks (A_1–A_4, S_1–S_4). At P_P of 2.17 kW, two anti-Stokes (A_1, A_2) and one Stokes (S_1) sidebands are obtained. At P_P of 2.67 kW, new discrete peaks at 419.7 nm (A_4) and 704.7 nm (S_4) have been observed. Narrow sidebands in the ultra-violet range at 390.7 nm (A_5) and 396.7 nm (A_6), far-detuned from the pump (~204 THz), have also been observed for the first time in SMF-28e + fiber at a PP of 4.61 kW. The possible explanation of such phenomena along with the theoretical predictions have been discussed extensively in our previous publication [23]. The further blue-shifting of the ultra-violet peak has also been achieved while exploring the IMFWM in a low-slope dispersion shifted fiber (HIPOSH, YOFC Ltd.) in a separate study by us [24]. The small core diameter, high index contrast and nonlinear mode coupling between the pump beams and the anti-Stokes wavelengths were found to be the reason for obtaining the UV peak at 341 nm at an input power of 3.89 kW. In the next section, we theoretically analyze the conditions for obtaining multiple IMFWM, and the spectral positions of the generated wavelengths under degenerate and non-degenerate pumping configurations.

3 Intermodal phase matching in communication fiber: Theoretical formulation

The SMF−28 fiber has a core diameter of 8.4 μm and is mainly used in long haul communication. The core (n_C) and cladding (n_{Cl}) refractive indices are related as, $n_C^2 \approx n_{Cl}^2 [1 + 2\Delta]$ with $\Delta \approx 0.3\%$. Although the fiber is single-moded for $\lambda \geq 1.31$ μm, it supports four spatial modes (excluding the polarization degeneracies) i.e. LP_{01}, LP_{11}, LP_{21} and LP_{02} at the operating wavelength of frequency-doubled Nd:YAG laser ($\lambda = 532$ nm) . In this section, we present the theoretical formulations for obtaining multiple intermodal four-wave mixing processes in such a fiber considering pump pulses in the nanosecond regime. One may note that the earlier papers had focused on the use of mode-locked pump pulses in the sub-picosecond regime [15]. However, the Q-switched lasers with nanosecond pulses, used in our work is much simpler, enabling savings in size and cost [6].

In IMFWM process, two pump photons propagate in different fiber modes simultaneously to generate one Stokes and one anti-Stokes photon either in the fundamental or in the higher order modes. The wavelength of the pump (λ_P), Stokes (λ_S) and anti-Stokes (λ_A) waves satisfy the energy conservation and phase matching (PM) conditions [8]:

$$\frac{2}{\lambda_P} = \frac{1}{\lambda_S} + \frac{1}{\lambda_A} \tag{1}$$

$$\Delta\beta = \beta_S^{l''m''}(\lambda_S) + \beta_A^{l'''m'''}(\lambda_A) - \beta_P^{lm}(\lambda_P) - \beta_P^{l'm'}(\lambda_P) = 0 \tag{2}$$

Here, $\beta_P^{lm}(\lambda_P)$, $\beta_P^{l'm'}(\lambda_P)$, $\beta_S^{l''m''}(\lambda_S)$ and $\beta_A^{l'''m'''}(\lambda_A)$ are the propagation constants of the pump, Stokes and anti-Stokes waves which belong to the LP_{lm}, $LP_{l'm'}$, $LP_{l''m''}$ and $LP_{l'''m'''}$ modes of the fiber. The evolution of the amplitudes of pump (A_{P_1}, A_{P_2}), Stokes (A_S) and anti-Stokes (A_A) fields is obtained by solving the coupled nonlinear Schrödinger equations as:

$$A_{P_1}(z) = A_{P_1}(0)\exp\left(i\gamma_{PP}(P_1 + 2P_2)z\right) \tag{3a}$$

$$A_{P_2}(z) = A_{P_2}(0)\exp\left(i\gamma_{PP}(P_2 + 2P_1)z\right) \tag{3b}$$

$$A_s(z) = \left[A_s(0)\{\cosh(gz) + i\frac{\kappa}{2g}\sinh(gz)\} + i\frac{\gamma_{SA}}{g}A_A^*(0)\sqrt{P_1P_2}\sinh(gz)\right]\exp i\left[\gamma_{SS}(P_1 + P_2) + \frac{\kappa}{2}\right]z \tag{3c}$$

$$A_A(z) = \left[A_A(0)\{\cosh(gz) + i\frac{\kappa}{2g}\sinh(gz)\} + i\frac{\gamma_{AS}}{g}A_S^*(0)\sqrt{P_1P_2}\sinh(gz)\right]\exp i\left[\gamma_{AA}(P_1+P_2) + \frac{\kappa}{2}\right]z \tag{3d}$$

Here, P_1 and P_2 are the pump powers in LP_{lm} and $LP_{l'm'}$ modes, respectively, $\kappa = \Delta\beta - (P_1 + P_2)[2(\gamma_{SS} + \gamma_{AA}) - 3\gamma_{PP}]$, and

$$g = \sqrt{\gamma_{SA}\,\gamma_{AS}\,P_1P_2 - (\kappa/2)^2}$$

$$\gamma_{ij} = \frac{3\omega_i\,\chi^{(3)}}{4\,\varepsilon_0 n_i^2\,c^2}\,\eta_{PPij}^{ll'\,l''\,l'''}$$

where, ω_P, ω_S and ω_A are frequencies of the pump, Stokes and anti-Stokes waves, respectively, n_i is the propagation constant at ω_i, $\chi^{(3)}$ is the third order susceptibility, and the nonlinear coupling η_{PPij}, that determines the conversion efficiency is defined as [8]:

$$\eta_{PPij}^{ll'\,l''\,l'''} = \int dA\; F_P^{lm} F_P^{l'm'} F_i^{l''m''*} F_j^{l'''m'''*} \tag{4}$$

$F_i^{lm}(r, \varphi)$ indicates the normalized field distribution of LP_{lm} fiber mode at λ_i and can be expressed as: $F_i^{lm}(r, \varphi) = F_i^{lm}(r) \exp(il\varphi)$. From the angular part of the overlap integral in Eq (4), one can obtain the following selection rule about the possible IMFWM processes [25]:

$$\eta_{PPij}^{ll'\,l''\,l'''} = 0 \qquad \text{for} \qquad l + l' - l'' - l''' \neq 0 \tag{5}$$

For these physically feasible IMFWM processes, the wavelength of the Stokes and anti-Stokes waves can be found by considering the Taylor series expansion of the propagation constants of Stokes and anti-Stokes waves i.e. $\beta_S^{l''m''}(\lambda_S)$ and $\beta_A^{l'''m'''}(\lambda_A)$ in Eq (2) around the pump frequency up to the second order as [19]:

$$\Delta\beta = \delta\beta^{(0)} + \delta\beta^{(1)}\,\Omega + \sum \beta^{(2)}\,\Omega^2 = 0 \tag{6}$$

where the spectral shifts Ω (in cm^{-1}), $\delta\beta^{(0)}$, $\delta\beta^{(1)}$ and $\Sigma\beta^{(2)}$ are defined as:

$$\Omega = \frac{1}{\lambda_P} - \frac{1}{\lambda_S} = \frac{1}{\lambda_A} - \frac{1}{\lambda_P} \tag{7}$$

$$\delta\beta^{(0)} = \beta_S^{l''m''}(\lambda_P) + \beta_A^{l'''m'''}(\lambda_P) - \beta_P^{lm}(\lambda_P) - \beta_P^{l'm'}(\lambda_P) \tag{8}$$

$$\delta\beta^{(1)} = 2\pi c\left[\beta_A^{l'''m'''(1)}(\lambda_P) - \beta_S^{l''m''(1)}(\lambda_P)\right] \tag{9}$$

$$\sum\beta^{(2)} = 2\pi^2 c^2\left[\beta_S^{l''m''(2)}(\lambda_P) + \beta_A^{l'''m'''(2)}(\lambda_P)\right] \tag{10}$$

Here, $\beta_i^{lm(n)}(\lambda_P) = \dfrac{\partial^n}{\partial\omega^n}\beta_i^{lm}(\lambda_P)$. The linear phase matching shift ($\Omega_{0\pm}$) can be expressed as the solution to Eq (6):

$$\Omega_{0+} = \frac{1}{2}\sqrt{\left(\frac{\delta\beta^{(1)}}{\Sigma\beta^{(2)}}\right)^2 - 4\,\frac{\delta\beta^{(0)}}{\Sigma\beta^{(2)}}} - \frac{\delta\beta^{(1)}}{2\Sigma\beta^{(2)}} \tag{11a}$$

$$\Omega_{0-} = -\frac{1}{2}\sqrt{\left(\frac{\delta\beta^{(1)}}{\Sigma\beta^{(2)}}\right)^2 - 4\,\frac{\delta\beta^{(0)}}{\Sigma\beta^{(2)}}} - \frac{\delta\beta^{(1)}}{2\Sigma\beta^{(2)}} \tag{11b}$$

For our work, $\Sigma\beta^{(2)}$ in Eq (10) is positive as the pump lies in the deep normal dispersion for all the supporting modes. The $\delta\beta^{(1)}$ in Eq (9) has small value (positive or negative) as both the modes possess identical β vs ω (or, λ) curves at λ_P. So, $\delta\beta^{(0)}$ in Eq (8) has to have significant negative values in order to achieve a large and real $\Omega_{0\pm}$ and hence feasible IMFWM. In the case when the two pump waves belong to the same mode

i.e. $l = l'$ and $m = m'$, Eqs (3c and 3d) would be modified slightly by assuming $P_1 = P_2$. Notably, in deriving Eqs (3a-3d), the contribution of linear mode coupling in PM condition has been ignored. This assumption is justified by considering the excitation of only three to four modes in a short length (few tens of cm) of host fiber free from any mechanical waveguide perturbation. We would also like to emphasize that although the frequency detuning of the generated sidebands in IMFWM and geometric parametric instability (GPI) in GRIN-MMF are quite similar, the mechanisms are completely different. Unlike IMFWM, the parametric instability process relies on the periodic self-imaging effect due to the excitation of large number of modes (more than 200) within the fiber [26].

4 Multiple intermodal four-wave mixing

In Fig 2, we have plotted the phase mismatch parameter ($\Delta\beta$) as a function of the spectral shift (Ω) for all possible IMFWM processes that satisfy Eq (5). The possible pump combinations are mentioned in the figure, whereas the modes of the corresponding Stokes and anti-Stokes are depicted in the inset. The position of $\Delta\beta(\Omega) = 0$ indicates the allowed IMFWM process and has been marked as $I_1 - I_6$ in Fig 2. Each IMFWM process in the positive Ω_0 (Ω_{0+}) side also has a complementary IMFWM in the negative Ω_0 (Ω_{0-}) having Stokes and anti-Stokes waves with interchanged mode-order. The spectral-shifts of all these processes, and the conversion efficiency along with the mode designation of the participating waves have been presented in Table 1. A slight asymmetry between each set of Ω_{0+} and Ω_{0-} occurs due to the presence of $\delta\beta^{(1)}$ in Eq (11) (see Table 1).

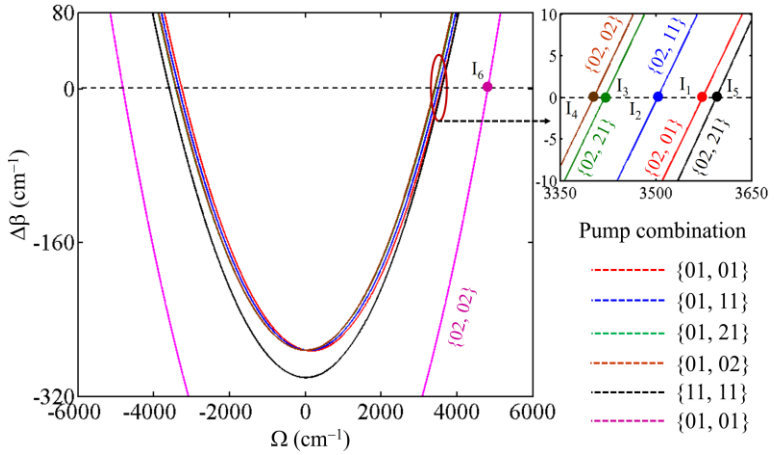

Fig 2. Phase-matched Stokes and anti-Stokes wavelengths in SMF-28 for different combinations of pump-mode.

In the case of the first four IMFWM processes (IMFWM #1: red − IMFWM #4: brown), the mode order of the anti-Stokes waves i.e. LP_{01}, LP_{11}, LP_{21}, LP_{02} coincides with one of the pump waves. Hence, the $\delta\beta^{(0)}$, in all these cases, would be simply the difference between the propagation constants of the LP_{02} Stokes mode ($LP_{l''m''}$) and fundamental pump mode (LP_{01}) i.e. 271.8 cm^{-1}. However, as one analyses the PM condition of IMFWM #1 and IMFWM #4, a decrease in Ω_{0+} (or, an increase in Ω_{0-}) is seen due to the decrement of $\delta\beta^{(1)}$ (see Eq 11) from -7.4×10^{-3} to zero. In IMFWM #5 (solid black curve) where both the pumps in LP_{11} mode completely annihilate to generate Stokes wavelength in LP_{02} and anti-Stokes in LP_{21} mode, an enhancement of the spectral shift (Ω_{0+} or, Ω_{0-}) was found. This is so because of the rise in $\delta\beta^{(0)}$ value to 300.3 cm^{-1} as the difference between the propagation constants of LP_{21} and LP_{11} is higher than that between LP_{11} and LP_{01}.

In IMFWM #6, where both the Stokes and anti-Stokes in LP_{02} mode are produced from the pump in LP_{01} mode, a significant detuning of generated sidebands from the pump is observed. An almost doubling

of $\delta\beta^{(0)}$ of this process in comparison to the previous IMFWM is responsible for such a huge upsurge in Ω_0 (I_6 in Fig 2). The difficulty in exciting both the pump-modes having dissimilar spatial field with almost equal intensity makes the IMFWM #1, #5, and #6 more favorable than the others. However, in a recent report by Ramachandran *et al*, the equal excitation of two circularly symmetric pump-modes (LP_{04} and LP_{05}) in a step-index MMF is achieved by using a binary phase plate encoded on a spatial light modulator [27]. Now, unlike in IMFWM #1 and IMFWM #6, where the excitation of the focused pump beam in LP_{01} mode can be achieved by carefully adjusting the input-end of the fiber using 3-D translational stage, the activation of IMFWM #5 requires launching the pump in LP_{11} modes. This, in general, can be achieved through a minute control over longitudinal (offset) as well as rotational (tilt) motion at the input by a five-axis positional stage with high precision [28].

Table 1. Comparison of spectral-shift and conversion efficiency of allowed IMFWM in SMF-28 under frequency-doubled Nd:YAG pumping

Process	P_1	P_2	Stokes	Anti-Stokes	F_{ijkl}^{mnop} ($\times 10^{-15} m^2$)	$\Omega_{0\pm}$ (cm^{-1})
IMFWM #1	LP_{01}	LP_{01}	LP_{02}	LP_{01}	13.5	3574
			LP_{01}	LP_{02}	11.5	−3256
IMFWM #2	LP_{01}	LP_{11}	LP_{02}	LP_{11}	0.7	3502
			LP_{11}	LP_{02}	3.0	−3333
IMFWM #3	LP_{01}	LP_{21}	LP_{02}	LP_{21}	4.0	±3419
			LP_{21}	LP_{02}	6.8	−3413
IMFWM #4	LP_{01}	LP_{02}	LP_{02}	LP_{02}	13.9	±3402
IMFWM #5	LP_{11}	LP_{11}	LP_{02}	LP_{21}	3.3	3594
			LP_{21}	LP_{02}	5.8	−3588
IMFWM #6	LP_{01}	LP_{01}	LP_{02}	LP_{02}	15.6	±4812

5 Cascaded intermodal four-wave mixing: Anti-Stokes pumping

In Fig 3, we have plotted the spectral shift as a function of pump detuning ($\Delta\Omega_P$) in cm^{-1} around 532 nm for the IMFWM #1 and IMFWM # 6 processes. It is clear from the figure that with an increase in frequency beyond the primary pump i.e. $\Delta\Omega_P$ is positive (blue shifted), the spectral shift reduces. But an increase in spectral shift occurs at the negative $\Delta\Omega_P$ side (red shifted) for both the processes. Here, one can extract the information about a complex cascaded IMFWM (C-IMFWM) which can be initiated by the above mentioned four wave mixing phenomena. In C-IMFWM process, the phase-matched Stokes and anti-Stokes waves act as the new secondary pump, and generate new secondary sidebands. This happens due to a significant transfer of energy from the primary pump to those of the primary sidebands. Such C-IMFWM is essential to produce narrow linewidth sources which are far detuned (more than 200 THz) from the main pump. In IMFWM #1, the phase-matched Stokes and anti-Stokes in LP_{02} and LP_{01} mode, respectively are found at $\Omega_{0+} = \Omega_1 = 3572$ cm^{-1} as indicated by point P in Fig 3. The pair of C-IMFWM triggered by this primary anti-Stokes can be found at $\Delta\Omega_P = \Omega_{0+}$ and marked as P_1 (Stokes in LP_{02}, anti-Stokes in LP_{01}) and P_2 (Stokes in LP_{01}, anti-Stokes in LP_{02}) with a spectral separation of 3013 cm^{-1} ($\Omega_{0+}{}^S$) and −2769 cm^{-1} ($\Omega_{0-}{}^S$), respectively. The overall positions of these secondary sidebands would be found at $\Delta\Omega_P \pm \Omega_{0+}{}^S$ (6585 cm^{-1}, 559 cm^{-1}) and $\Delta\Omega_P \pm \Omega_{0-}{}^S$ (6343 cm^{-1}, 803 cm^{-1}) from the primary pump. The C-IMFWM initiated by the primary Stokes wave in LP_{02} mode at $\Delta\Omega_P = -\Omega_{0+}$ has not been found feasible as the corresponding PM curve remains positive in the entire visible range for all the IMFWM processes that satisfy the selection rule (Eq 5). This reason also holds

for not generating any C-IMFWM assisted sidebands due to the primary anti-Stokes wave in LP_{02} mode of the other set of IMFWM #1 process (Stokes in LP_{01}, anti-Stokes in LP_{02}) at $\Delta\Omega_P = -\Omega_{0-} = 3256\ cm^{-1}$. However, the scenario is different in the case of a pair of cascaded processes triggered by the Stokes line at $\Delta\Omega_P = \Omega_{0-}$. Here, the secondary sidebands are found to have a spectral shift of 3955 cm^{-1} ($\Omega_{0+}^{S'}$) and −3783 cm^{-1} ($\Omega_{0-}^{S'}$) and marked by Q_1 (Stokes in LP_{02}, anti-Stokes in LP_{01}) and Q_2 (Stokes in LP_{01}, anti-Stokes in LP_{02}), respectively. The first set does not imply a physically acceptable solution as the overall spectral position of the secondary Stokes i.e. $\Delta\Omega_P - \Omega_{0+}^{S'}$ (−7211 cm^{-1}) from the primary pump lies beyond the LP_{02} mode cut-off, which is at −6030 cm^{-1} from $\lambda_P = 532$ nm. But the second set denotes a valid C-IMFWM with the generated Stokes and anti-Stokes at $\Delta\Omega_P \pm \Omega_{0-}^{S}$ (−7039 cm^{-1}, −527 cm^{-1}) around the initial pump.

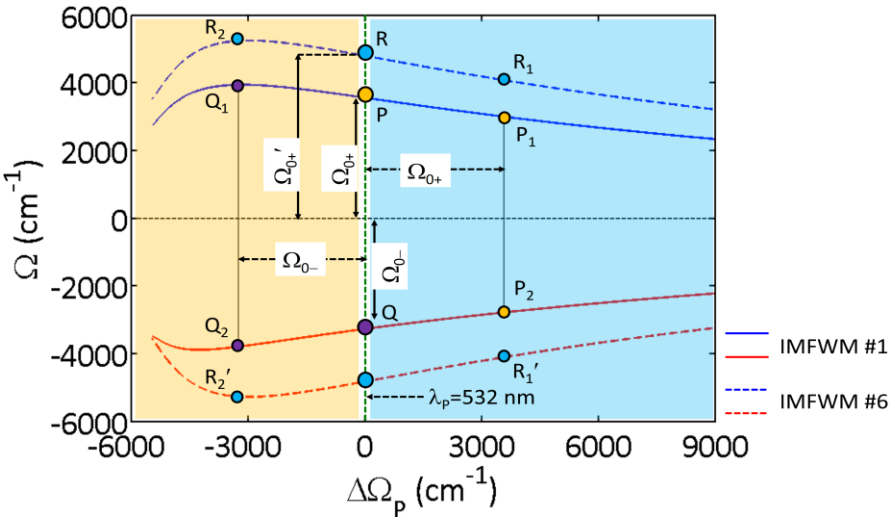

Fig 3. Cascaded intermodal phase-matching in SMF-28 for different secondary pump configuration.

Note that, all the possible C-IMFWM discussed above belong to the IMFWM #1 (Stokes in LP_{02}, anti-Stokes in LP_{01} or vice versa) category. However, the cascaded process which belongs to the IMFWM # 6 and which is produced by the same secondary anti-Stokes and Stokes at $\Delta\Omega_P = \Omega_{0+}$ and $\Delta\Omega_P = -\Omega_{0-}$, respectively is not allowed. This is so because the generated secondary sidebands (marked as R_1, R_1', R_2 and R_2'), all in LP_{02}, once again belong to the non-guided radiative modes. It may be noted that, similar to the case of primary Stokes in LP_{02} at $\Delta\Omega_P = -\Omega_{0+}$ or, the primary anti-Stokes in LP_{02} at $\Delta\Omega_P = -\Omega_{0-}$, the primary Stokes (or, anti-Stokes) at Ω_{0+}' in LP_{02} of IMFWM # 6 (marked as R in Fig 2) cannot initiate any C-IMFWM process.

6 Conclusion

We performed a thorough investigation on the possible generation of far detuned discrete wavelengths from ultraviolet to visible range using multiple IMFWM processes in SMF-28e+ fiber if it is pumped with a low power quasi-continuous wave laser in the normal dispersion region. A numerical analysis, based on the solution of the coupled nonlinear Schrödinger equation under undepleted pump approximation, is carried out to explore various classes of IMFWM phenomena under different pump mode excitations. The cascaded IMFWM as a result of secondary pumping to generate narrowband sources in the ultraviolet regime is also investigated. Being close to the pump, the spontaneous Raman scattering peak bears no effect on the generated sidebands. The intermodal walk-off is also found to be negligible (40 fs/cm at 532 nm) for the input pulse in the nanosecond/picosecond regime. We expect our results on the generation of a pair of Stokes/

anti-Stokes lines, far-detuned from the pump i.e. 3500−4800 cm^{-1}, would be useful in quantum information processing technologies [27] as well as in biomedical science and fluorescence spectroscopy.

Acknowledgements

Dr Sudip Kumar Chatterjee acknowledges the Centre for Lasers and Photonics, Indian Institute of Technology Kanpur for providing the institute post-doctoral fellowship and the Pulsed laser facility for the laboratory access to carry out the research work.

References

1. Stolen R H, Bjorkholm J E, Ashkin A, Phase-matched three-wave mixing in silica fiber optical waveguides, *Appl* Phys Lett, 24(1974)308–310.
2. Dudley J M, Genty G, Coen S, Supercontinuum generation in photonic crystal fiber, *Mod Phys*, 78(2006)1135–1184.
3. Stolen R H, Bjorkholm J E, Parametric amplification and frequency conversion in optical fibers, *IEEE J Quantum Electron*, 18(1982)1062–1072.
4. de Brito D B, Ramos R V, Analysis of heralded single-photon source using four-wave mixing in optical fibers via wigner function and its use in quantum key distribution, *IEEE J Quantum Electron*, 46(2010)721–727.
5. McKinstrie C J, Mejling L, Raymer M G, Rottwitt K, Quantum-state-preserving optical frequency conversion and pulse reshaping by four-wave-mixing, *Phys Rev* A, 85(2012)053829; doi.org/10.1103/PhysRevA.85.053829.
6. Wadsworth W J, Joly N, Knight J C, Birks T A, Biancalana F, Russell P St J, Supercontinuum and four-wave mixing with Q-switched pulses in endlessly single-mode photonic crystal fibres, *Opt Express*, 12(2004)299–309.
7. Konorov S O, Serebryannikov E E, Zheltikov A M, Zhou P, Tarasevitch A P, von der Linde D, Generation of femtosecond anti-Stokes pulses through phase-matched parametric four-wave mixing in a photonic crystal fiber, *Opt Lett*, 29(2004)1545–1547.
8. Agrawal G P, Nonlinear Fiber Optics, 4th Edn, (Academic Press, Boston), 2007.
9. Lin Q, Yaman F, Agrawal G P, Photon-pair generation in optical fibers through four-wave mixing: Role of Raman scattering and pump polarization, *Phys Rev* A, 75(2007)023803; doi.org/10.1103/PhysRevA.75.023803.
10. Van der Westhuizen G, Nilsson J, Fiber optical parametric oscillator for large frequency-shift wavelength conversion, *IEEE J Quantum Electron*, 46(2010)721–727.
11. Rarity J G, Fulconis J, Duligall J, Wadsworth W J, Russell P St J, Photonic crystal fiber source of correlated photon pairs, *Opt Express*, 13(2005)534–544.
12. Tu H, Jiang Z, Marks D L, Boppart S A, Intermodal four-wave mixing from femtosecond pulse-pumped photonic crystal fiber, *Appl Phys Lett*, 94(2009)101109; doi.org/10.1063/1.3094127.
13. Mafi A, Pulse propagation in a short nonlinear graded-index multimode optical fiber, *J Lightwave Technol*, 30(2012)2803–2811.
14. Cheng J, Pedersen M E V, Charan K, Wang K, Xu C, Gruner-Nielsen L, Jakobsen D, Intermodal four-wave mixing in a higher-order-mode fiber, *Appl Phys Lett*, 101(2012)161106; doi.org/10.1063/1.4759038.
15. Yuan J, Sang X, Wu Q, Zhou G, Li F, Zhou X, Yu C, Wang K, Yan B, Han Y, Tam H Y, Wai P K A, Enhanced intermodal four-wave mixing for visible and near-infrared wavelength generation in a photonic crystal fiber, *Opt Lett*, 40(2015)1338–1341.
16. Nazemosadat E, Pourbeyram H, Mafi A, Phase matching for spontaneous frequency conversion via four-wave mixing in graded-index multimode optical fibers, *J Opt Soc Am B*, 33(2016)144–150.
17. Bendahmane A, Krupa K, Tonello A, Modotto D, Sylvestre T, Couderc V, Wabnitz S, Millot G, Seeded intermodal four-wave mixing in a highly multimode fiber, *J Opt Soc Am B*, 35(2018)295–301.
18. Pourbeyram H, Mafi A, Photon pair generation in multimode optical fibers via intermodal phase matching, *Phys Rev* A, 94(2016)023815; doi.org/10.1103/PhysRevA.94.023815
19. Pourbeyram H, Nazemosadat E, Mafi A, Detailed investigation of intermodal four-wave mixing in SMF-28: blue-red generation from green, *Opt Express*, 23(2015)14487–14500.

20. Demas J, Steinvurzel P, Tai B, Rishoj L, Chen Y, Ramachandran S, Intermodal nonlinear mixing with Bessel beams in optical fiber, *Optica*, 2(2015)14–17.
21. Dupiol R, Bendahmane A, Krupa K, Tonello A, Fabert M, Kibler B, Sylvestre T, Barthelemy A, Couderc V, Wabnitz S, Millot G, Far-detuned cascaded intermodal four-wave mixing in a multimode fiber, *Opt Lett*, 42(2017)1293–1296.
22. Yuan J, Kang Z, Li F, Zhang X, Mei C, Zhou G, Sang X, Wu Q, Yan B, Zhou X, Zhong K, Wang K, Yu C, Farrell G, Lu C, Tam H Y, Wai PKA, Experimental Generation of Discrete Ultraviolet Wavelength by Cascaded Intermodal Four-Wave Mixing in a Multimode Photonic Crystal Fiber, *Opt Lett*, 42(2017)3537–3540.
23. Chatterjee S K, Vijaya R, Degenerate intermodal four-wave mixing with Q-switched nanosecond pulses in SMF-28 for the generation of discrete ultraviolet-visible wavelengths, *OSA Continuum*, 1(2018)1360–1369.
24. Chatterjee S K, Vijaya R, Narrowband ultraviolet generation in dispersion-shifted few-mode fiber via combined effect of intermodal four-wave mixing and nonlinear mode coupling, Opt Commun, 458(2020)124816; doi.org/10.1016/j.optcom.2019.124816.
25. Poletti F, Horak P, Description of ultrashort pulse propagation in multimode optical fibers, *J Opt Soc Am B*, 25 (2008)1645–1654.
26. Krupa K, Tonello A, Barthelemy A, Couderc V, Shalaby B M, Bendahmane A, Millot G, Wabnitz S, Observation of Geometric Parametric Instability Induced by the Periodic Spatial Self-Imaging of Multimode Waves, *Phys Rev Lett*, 116(2016)183901; doi.org/10.1103/PhysRevLett.116.183901.
27. Demas J, L. Rishøj, X Liu, G. Prabhakar, and S. Ramachandran, "High-power, wavelength-tunable NIR all-fiber lasers via intermodal four- wave mixing", CLEO: Applications and Technology, JTh5A, California, USA, May 2017.
28. Khan S N, Chatterjee S K, Chaudhuri P R, Polarization and propagation characteristics of switchable first-order azimuthally asymmetric beam generated in dual-mode fiber, *Appl Opt*, 54(2015)1528–1542.

[*Received*: 27.11.2021; *accepted*: 05.12.2021]

Dr Sudip Kumar Chatterjee is currently an Assistant Professor in the department of Physics at Bennett University. Prior to his present appointment, he worked as a postdoctoral fellow in the department of Instrumentation and Applied Physics, Indian Institute of Science Bangalore during 2020-2021, at Indian Institute of Technology Kanpur during 2017-2020, and at Indian Institute of Technology Kharagpur during 2016-2017. He received his doctoral degree from Indian Institute of Technology Kharagpur in 2016. His research interests include Nonlinear parametric processes, Beam manipulation in fiber, and Advanced interferometric sensors.

Professor Vijaya is an experimental physicist working in topics related to Optics and Photonics for the past 30 years. After completing her doctoral degree and CSIR research associateship at IIT Madras, she worked at SSSIHL for 4 years

and IIT Bombay for 14 years, before she moved to IIT Kanpur in 2011. Her research work includes nonlinear optics, fiber optics, nanophotonics, optical devices, miniature lasers, microstrip patch antennas and metasurfaces, all with an emphasis on applications. Apart from teaching and research, outreach effort for school and undergraduate education is one of her passions. She is a senior member of IEEE, Optica and SPIE.